Nuclear Instruments and Methods in Physics Research B 267 (2009) 1518–1521

Contents lists available at ScienceDirect

Nuclear Instruments and Methods in Physics Research B

journal homepage: www.elsevier.com/locate/nimb

Effects of ion irradiation in metallic glasses

Jesse Carter [a], E.G. Fu [b], G. Bassiri [c], B.M. Dvorak [c], N. David Theodore [d], Guoqiang Xie [e], D.A. Lucca [c], Michael Martin [a], Mark Hollander [a], Xinghang Zhang [b], Lin Shao [a,*]

[a] Department of Nuclear Engineering, Texas A&M University, 129 Zachry, 3133 TAMU, College Station, TX 77843, USA
[b] Department of Mechanical Engineering, Texas A&M University, College Station, TX 77843, USA
[c] School of Mechanical and Aerospace Engineering, Oklahoma State University, Stillwater, OK 74078, USA
[d] Silicon Technology Solutions, Freescale Semiconductor Inc., Tempe, AZ 85284, USA
[e] Institute for Materials Research, Tohoku University, Sendai 980-8577, Japan

ARTICLE INFO

Article history:
Available online 30 January 2009

PACS:
61.66.Dk
61.80.–x
61.82.Bg

Keywords:
Ion irradiation
Metallic glass
High strength alloy
Nanoindentation
Microindentation

ABSTRACT

Application of metallic glasses as structural materials has been limited by their poor ductility. To overcome brittle failure, nanocrystals are intentionally introduced to stabilize the glasses. In this study, we report on the application of ion irradiation to induce nanocrystalization in a $Cu_{50}Zr_{45}Ti_5$ (CZT) alloy. Transmission electron microcopy, microindentation and nanoindentation have been used to characterize the CZT alloy irradiated with 140 keV He ions at room temperature. Hardness enhancement was observed near the projected range of the He ions, coinciding with the formation of nanocrystals. Such microstructural changes, however, were not observed in the near surface region, where the electronic stopping process is dominant.

1. Introduction

Metallic glasses possess unique chemical and mechanical properties due to a lack of crystal defects [1]. They can be used as structural materials under aggressive environments requiring high strength and high corrosion resistance. However, their application has been limited by their poor ductility. Recently, it has been suggested that this issue can be alleviated if the metallic glass contains nanocrystals – crystals with diameters of a few nanometers [1–4].

Various approaches have been proposed to form nanocrystals in metallic glasses [5]. The most straightforward method is to heat the material at an elevated temperature, but this method only works in certain metallic glasses [5]. Other approaches include electron irradiation [6–9] and ion irradiation [10]. Oriented nanocrystals have been observed after ion irradiation of a Ni–P alloy by using a focused Ga ion beam [10]. However, the details of this mechanism are not clear.

In this study, we aimed at using a relatively high energy ion beam to modify the mechanical properties of metallic glasses by avoiding the surface effect hypothesized in previous studies [10].

2. Experimental procedure

Our study began with preparing a $Cu_{50}Zr_{45}Ti_5$ alloy by melting mixtures of pure Cu, Zr and Ti in an argon atmosphere [9]. Ribbon-shaped samples, 1.5 mm in width and about 20 μm thick, were obtained by rapid solidification of the melt on a single copper roller at a peripheral velocity of 42 m/s in an argon atmosphere. The sample was cut into pieces and irradiated at room temperature with 140 keV He ions to a fluence of $1.7 \times 10^{17}/cm^2$. Implantation of He atoms was motivated by the need to form high strength porous materials with enhanced mechanical properties and reduced weight. We selected 140 keV as the implantation energy primarily due to the feasibility of the accelerator instruments. The homemade accelerator was optimized for this energy. Beam heating was measured to be less than 50 °C. Nanoindentation tests were performed on both specimens (as-spun and irradiated) in order to obtain the distribution of hardness as a function of depth. Due to the thickness and curvature of the specimens, it was necessary

* Corresponding author. Tel.: +1 979 845 4107; fax: +1 979 845 6443.
E-mail address: lshao@mailaps.org (L. Shao).

0168-583X/$ - see front matter © 2009 Elsevier B.V. All rights reserved.
doi:10.1016/j.nimb.2009.01.081

to mount the specimens onto a microscope slide using superglue to ensure proper measurements. Due to the limitation of the maximum penetration depth in the nanoindentation tests, microindentation tests were also performed using a Fischerscope HM2000 with a Vicker's indenter. Irradiation induced hardness changes were extracted by comparing data before and after ion irradiation. Depth dependent hardness changes were discussed and compared with stopping powers of He ions, obtained by using the Stopping and Range of Ions in Matter (SRIM) code [11]. High resolution transmission electron microscopy (TEM) was performed to characterize the samples.

3. Results and discussion

The values for hardness as a function of contact depth for both as-spun and irradiated specimens, are shown in Fig. 1. A set of five loads were initially utilized in order to determine the distribution of hardness. In order to obtain the greatest possible depth profile, an additional load was added (10,000 μN). Each data point in Fig. 1 represents the average hardness value for five indentation measurements at each load and the error bars represent the maximum and minimum values obtained. As shown in Fig. 1, there are no significant hardness changes from the surface up to 250 nm.

Fig. 2 shows the hardness in both the as-spun and irradiated metallic glass samples obtained by using microindentation. At a depth of around 600 nm, the hardness increases from 9 GPa (as-spun) to 12 GPa in the irradiated samples. The hardness change becomes much smaller at depths beyond 1000 nm. Different from the nanoindentation tests, which give more reliable data in the near surface region, hardness data obtained by microindentation is not reliable for depths shallower than ~200 nm. Hardness changes observed at a depth of approximately 600 nm, as shown in Fig. 2, indicate a significant mechanical property change in the ion irradiated metallic glasses.

Fig. 3 shows the hardness changes extracted from the data in Fig. 2. Hardness enhancement in the irradiated sample reaches a peak at a depth of around 600 nm. The trend of the curve from 300 to 600 nm suggests that hardness enhancement is negligible for shallow depths (<300 nm). This observation is consistent with the data obtained by nanoindentation.

It is well known that the contribution to ion stopping in solids originates from two different mechanisms – nuclear and electronic

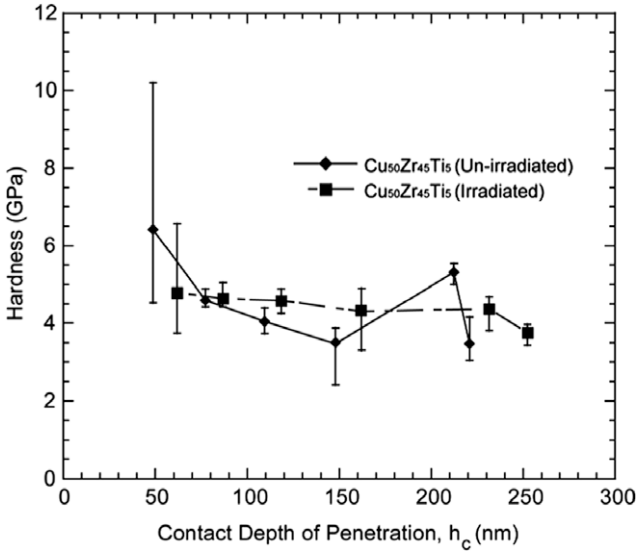

Fig. 1. Plot of indentation hardness of unirradiated and irradiated $Cu_{50}Zr_{45}Ti_5$ metallic glass samples versus contact depth obtained from nanoindentation.

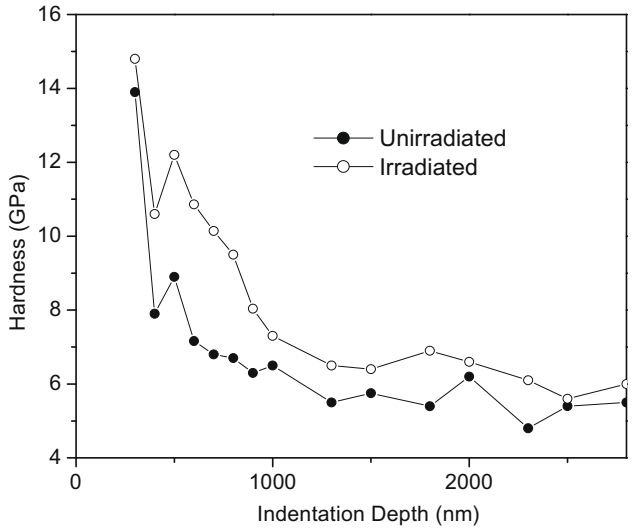

Fig. 2. Plot of indentation hardness of unirradiated and irradiated $Cu_{50}Zr_{45}Ti_5$ metallic glass samples versus indentation depth obtained from microindentation.

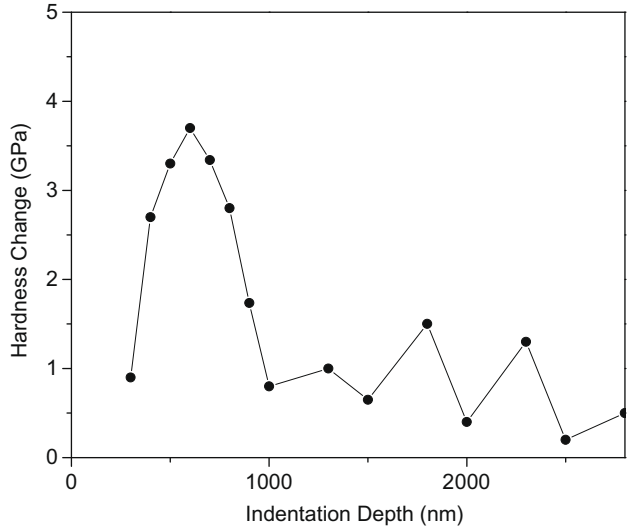

Fig. 3. Hardness changes between unirradiated and irradiated metallic glass. The data is calculated based on Fig. 2.

stopping [12]. In nuclear stopping, ions lose energy by ion-target nuclear collisions; in electronic stopping, ions lose energy by collision with target electrons. The relative importance of these two stopping mechanisms depends on the velocity and charge state of the ions. Fig. 4 compares electronic and nuclear stopping powers of He ions in the sample. SRIM does not directly provide stopping powers as a function of depth. We first used SRIM to calculate stopping powers as a function of energy. Then the energy was converted into the corresponding depth for 140 keV He ions. As shown in Fig. 4, electronic stopping decreases with increasing depths, while nuclear stopping peaks at a depth of ~600 nm, which corresponds to the projected range of 140 keV He ions in this metallic glass. Our study suggests that the hardness enhancement is due to either the nuclear stopping process or implanted He atoms, and the electronic stopping process is not playing a dominant role in the mechanical property changes.

Fig. 5 shows a dark-field TEM image of the unirradiated metallic glass. No nanocrystalline particles are observed. The selected area diffraction (SAD) pattern further confirms its amorphous phase.

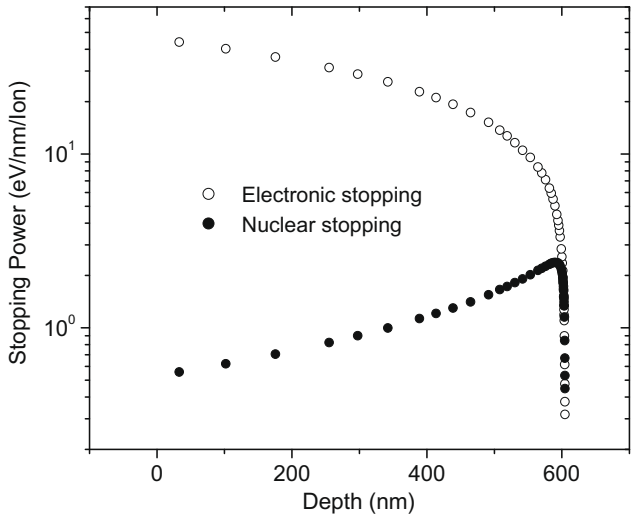

Fig. 4. A comparison of nuclear stopping and electronic stopping as a function of penetration depth in the metallic glass for 140 keV He ions. The data is calculated using SRIM code.

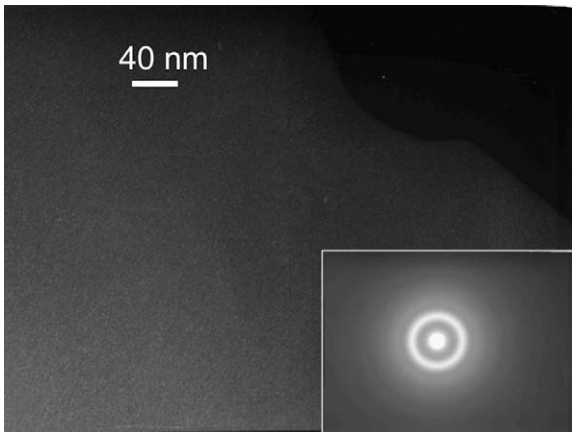

Fig. 5. Dark-field TEM image of the unirradiated metallic glass. The inset represents the corresponding selected area diffraction pattern.

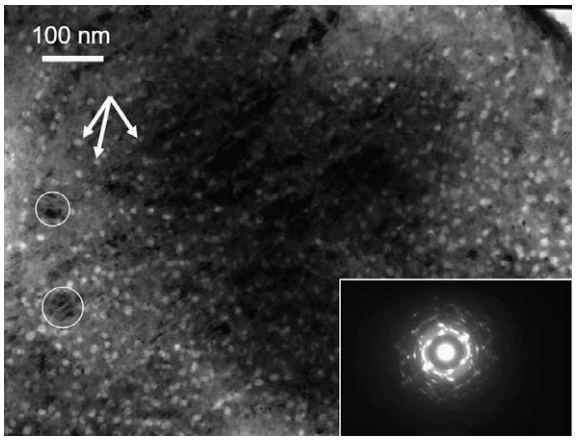

Fig. 6. Bright-field TEM image of the irradiated metallic glass. The inset represents the corresponding selected area diffraction pattern.

In comparison, Fig. 6 shows a bright-field TEM of the irradiated sample. The bright spots (as indicated by arrows) correspond to helium bubbles and/or voids formed in the sample. It is difficult to distinguish one from the other since both types of defects are open volume defects. Such defects are frequently observed in gas-atom-irradiated alloys [13]. The half width of 140 keV He implant distribution is around 100 nm. If all implanted He atoms are retained at the end of their ranges, the He concentration near the peak region is estimated to be around 6×10^{21} atoms/cm^3. Circles in Fig. 6 refer to typical nanocrystalline particles. The crystallites have irregular shapes and sizes ranging from a few nanometers up to 100 nm. Nanocrystal formation is further confirmed by the SAD pattern (the inset in Fig. 6) and dark-field TEM (not shown here).

Limited studies have shown that the dispersion of nanocrystals in an amorphous matrix can lead to dispersion strengthening of the materials [14,15]. Therefore, it is expected that the yield strength will increase as a function of the volume fraction of nanocrystals [16]. We hypothesize that nanocrystal formation is related to damage cascade formation. Development of the damage cascade is a very complicated process. Basically, after the initial damage cascade and associated thermal spike formation, the core of the cascade forms a "liquid-like" hot zone. The zone is virtually cooled to an ambient temperature after a "quenching" process. During quenching, energy is dissipated via lattice vibrations [12]. Damage cascade formation may involve phase separation and asymmetric diffusion between different elements. Significant energy deposition associated with the formation of a melting zone is equivalent to localized high temperature heating. This local heating can cause chemical decomposition and periodic composition fluctuations which give rise to nanocrystal formation. However, it is worthy to point out that the cooling rate after thermal spike is certainly faster than cooling rate of the initial quench. Even if the material has localized melting, it does not necessarily lead to nanocrystal formation. It is possible that nanocrystal formation is due to enhanced mobility of atoms under irradiation. The mechanisms are not clear at this stage.

Gas atom implantation, such as the He implantation used in this study, could be used for development of porous high strength alloy coatings. A conclusive explanation of the mechanisms responsible for hardness changes is difficult in the case of gas atom implantation since such hardness changes can be influenced by both nanocrystal formation and bubble formation. In order to know their relative contributions, self ion irradiation into metallic glass is necessary. Such experiments are currently being undertaken by us.

4. Summary

We have studied ion irradiation induced hardness changes in a $Cu_{50}Zr_{45}Ti_5$ (CZT) alloy. After 140 keV He ion irradiation to a fluence of 1.7×10^{17}/cm^2, a maximum in hardness enhancement occurs at a depth close to the maximum nuclear stopping and projected range of the implants. TEM studies have identified nanocrystals formed in the irradiated metallic glasses.

Acknowledgement

This work was financially supported by the University Embryonic Technologies Program from Siemens Power Generation Emerging Technologies. L. Shao acknowledges the support from the NRC Early Career Development Grant. X. Zhang acknowledges the support by DOE under grant number DE-FC07-05ID14657.

References

[1] A. Inoue, Acta Mater. 48 (2000) 279.
[2] M.X. Xia, C.L. Ma, H.X. Zheng, J.G. Li, Mater. Sci. Eng. A 390 (2005) 372.
[3] S.W. Lee, M.Y. Huh, E. Fleury, J.C. Lee, Acta Mater. 54 (2006) 349.
[4] D.V. Louzguine, A. Inoue, J. Nanosci. Nanotechnol. 5 (2005) 999.
[5] S. Schneider, P. Thiyagarajan, W.L. Johnson, Appl. Phys. Lett. 68 (1996) 493.

[6] X.W. Du, M. Takeguchi, M. Tanaka, K. Furuya, Appl. Phys. Lett. 82 (2003) 1108.
[7] T. Nagase, Y. Umakoshi, Mater. Trans. 46 (2005) 616.
[8] A. Nino, T. Nagase, Y. Umakoshi, Mater. Trans. 46 (2005) 1814.
[9] G. Xie, Q. Zhang, D.V. Louzguine-Luzgin, W. Zhang, A. Inoue, Mater. Trans. 47 (2006) 1930.
[10] R. Tarumi, K. Takahima, Y. Higo, Appl. Phys. Lett. 81 (2002) 4610.
[11] J.F. Ziegler, J.P. Biersack, U. Littmark, The Stopping and Range of Ions in Solids, Pergamon, New York, 1985.
[12] M. Nastasi, J.W. Mayer, J.K. Hirvonen, Ion–Solid Interaction: Fundamentals and Applications, Cambridge University Press, UK, 1996.
[13] G.S. Was, Fundamentals of Radiation Materials Science, Springer, New York, 2007.
[14] A. Leonhard, L.Q. Xing, M. Heilmaier, A. Gebert, J. Eckert, L. Schultz, Nanostruct. Mater. 10 (1998) 805.
[15] B.M. Clemens, H. Kung, S.A. Barnett, MRS Bull. 24 (1999) 20.
[16] G. Fan, A. Inoue, Appl. Phys. Lett. 77 (2000) 46.